

Dissipative hydrodynamics coupled to chiral fields

J. Peralta-Ramos* and G. Krein†

*Instituto de Física Teórica, Universidade Estadual Paulista,
Rua Doutor Bento Teobaldo Ferraz, 271 - Bloco II, 01140-070 São Paulo, SP, Brazil*

Using second-order dissipative hydrodynamics coupled self-consistently to the linear σ model we study the 2 + 1 dimensional evolution of the fireball created in Au+Au relativistic collisions. We analyze the influence of the dynamics of the chiral fields on the charged-hadron elliptic flow v_2 and on the ratio $v_4/(v_2)^2$ for a temperature-independent as well as for a temperature-dependent viscosity-to-entropy ratio η/s calculated from the linearized Boltzmann equation in the relaxation time approximation. We find that v_2 is not very sensitive to the coupling of chiral sources to the hydrodynamic evolution, but the temperature dependence of η/s plays a much bigger role on this observable. On the other hand, the ratio $v_4/(v_2)^2$ turns out to be much more sensitive than v_2 to both the coupling of the chiral sources and the temperature dependence of η/s .

I. INTRODUCTION

One of the most surprising outcomes of the experiments conducted at the Relativistic Heavy Ion Collider (RHIC) is the discovery that high-energy collisions of heavy ions produce strongly interacting hadronic matter (quark-gluon plasma – QGP) that evolves as a low-viscosity fluid [1–6]. This came as a surprise because early expectations, motivated mainly by the asymptotic freedom property of Quantum Chromodynamics (QCD), were that RHIC would create a gas-like system of weakly interacting quarks and gluons.

The strongly interacting nature of the QGP is revealed through the description of measured momentum anisotropies via relativistic viscous hydrodynamics calculations. The momentum anisotropies are encoded in the Fourier moments v_2, v_3, v_4, \dots of the measured azimuthal distribution of particles, and are interpreted as being the translation to momentum space of the initial spatial eccentricity of non central collisions [7]. A weakly-interacting, gas-like fluid would have no mechanism to induce such a translation into momentum anisotropies, but they can be produced if the particles of the fluid are strongly interacting.

In any attempt of describing experimental results of a heavy ion collision via a viscous hydrodynamics model, crucial physics input reflecting the properties of the flowing hadronic matter must be supplemented, like the equation of state (EOS) and transport coefficients, as shear (η) and bulk (ζ) viscosities. Although it is expected that for the strongly-coupled QGP η and ζ will depend strongly on temperature – see below – usually in hydrodynamic simulations temperature-independent values for these coefficients are assumed throughout the entire evolution. The impact of the temperature dependence of transport coefficients on momentum anisotropies that are obtained from hydrodynamic models has been recently

investigated in Refs. [8–14].

These transport coefficients are, in principle, derivable from first-principles QCD calculations at finite temperature, but in practice, the calculations are extremely difficult at strong coupling. There is a long history of computations of the EOS via large-scale numerical simulations of QCD on a lattice and modern calculations are achieving the accuracy needed for reliable use in heavy-ion physics – for a recent overview on the subject, see Ref. [15]. On the other hand, lattice QCD calculations of transport coefficients are still in their infancy and only recently have results for shear and bulk viscosities been obtained [16–18]. Analytically, calculations have been performed within QCD for the shear and bulk viscosities [19, 20] at extremely high temperatures, where perturbation theory in the coupling constant can be used on account of asymptotic freedom. Reliable calculations for these quantities can also be done at very low temperatures, where matter consists essentially of a very dilute gas of pions. There is plenty of experimental information on elementary low-energy hadron-hadron interactions available that can be used to constrain detailed calculations that go beyond lowest-order in chiral perturbation theory [21, 22]. On the other hand, in the region of intermediate temperatures, $T \sim \Lambda_{QCD}$, where one expects the deconfinement and chiral transitions to occur [23], perturbative expansions (in the coupling constant or chiral) are not applicable. There is lack of experimental information on the appropriate degrees of freedom to use and phenomenological approaches are an alternative, like the use of relativistic kinetic theory [24–30].

Assuming the validity of a relativistic viscous hydrodynamical description, experimental extraction of transport coefficients should be possible in principle from comparison with measured momentum anisotropy patterns. Moreover, as suggested in Ref. [31], such a comparison with experimental data would allow to pinpoint the location of the QCD phase transition or of a crossover from hadronic to quark-gluon matter. In this context, in addition to the hydrodynamic degrees of freedom related to energy-momentum conservation, degrees of freedom associated with order parameters of broken continuous

*jperalta@ift.unesp.br

†gkrein@ift.unesp.br

symmetries must be considered as well since they are all coupled to each other. Particularly important to the quest of determining possible signals of the chiral transition is the coupling of chiral fields to the fluid-dynamical modes. The present work is a first step towards the study of effects of such a coupling on momentum anisotropies within a viscous hydrodynamic description.

Specifically, in the present paper we study, in the context of second-order dissipative relativistic hydrodynamics, the influence of the long-wavelength modes of chiral fields on the expansion of the fireball created in Au+Au collisions at $\sqrt{s_{NN}} = 200$ GeV. In particular, we aim at studying the effect of the coupled evolution of chiral degrees of freedom on the flow asymmetry characterized by v_2 and $v_4/(v_2)^2$, when finite viscosity is taken into account within a simple microscopic model for the chiral condensate.

In our model the flowing matter consists of a fluid of quarks and antiquarks in local thermal equilibrium that evolves according to a second-order dissipative hydrodynamic model [32–34] with temperature-dependent speed of sound and transport coefficients. Starting from a high temperature state with approximately restored chiral symmetry, the system is evolved towards a state where the symmetry is spontaneously broken. The quark-antiquark fluid interacts locally with the chiral fields of the linear σ model (LSM) [35]. We compare the results obtained for hadronic observables when the chiral fields are included or not as sources in the hydrodynamic equations.

Similar models for the dynamics of quarks coupled to chiral fields were considered before. Mishustin and Scavini [36] constructed a relativistic mean field *ideal* fluid dynamical model based on the LSM, while Abada and Birse [37] used the Vlasov equation to describe the quarks coupled to the LSM. Both studies focused on the evolution of the chiral fields rather than on the influence of their dynamics on hadronic observables, which is the main focus here. Son [38] and Pujol and Davesne [39] have developed modified hydrodynamic theories including additional (chiral) symmetry-breaking hydrodynamic variables, which were subsequently applied by Lallouet et al. [40] to the study of Bjorken flow in heavy-ion collisions. Later on, Paech et al. [41, 42] coupled 3+1 *ideal* hydrodynamics to the LSM including fluctuations of the chiral fields and studied the behavior of the azimuthal momentum asymmetry at nonzero impact parameter. More recently, Nahrgang and Bleicher [43] included phenomenological dissipation and noise terms in the equation of motion of the σ field of the LSM coupled to ideal hydrodynamics. They focused on sigma fluctuations and found that at the first order phase transition they lead to an increase in the intensity of sigma excitations. In a subsequent work, Nahrgang, Leupold, Herold and Bleicher [44] employed the two-particle irreducible (2PI) effective action formalism to set up an approximation scheme to derive explicit formulas for the dissipation kernel and the noise correlation function within

the LSM. While the approximations employed deserve careful scrutiny, the formulas derived within the mentioned approximation scheme show interesting features of dissipation and noise on the relaxation dynamics of the chiral dynamics and point to the importance of including reheating of the quark fluid by energy dissipation from the chiral fields, as shown in the very recent papers by Nahrgang, Leupold and Bleicher [45] and Nahrgang, Bleicher, Leupold, and Mishustin [46]. The work of Plumari et al. [47] is more in the spirit of ours in the present paper, in that they have investigated the role of the chiral transition on v_2 . Specifically, the authors have solved numerically the Boltzmann–Vlasov transport equations including both two-body collisions and the chiral phase transition as given by the Nambu–Jona-Lasinio model. For conditions prevailing in Au + Au collisions at $\sqrt{s_{NN}} = 200$ GeV, the authors find a sizable suppression of v_2 due to the attractive nature of the chiral field dynamics. They also found that, if η/s is kept fixed, v_2 does not depend on the details of the collisional and/or field dynamics and in particular it is not affected significantly by the chiral phase transition.

At this point it is appropriate to state the limited scope of our work. First of all, while we use a viscous hydro model coupled to a workable chiral model, we do not intend to extract values of transport coefficients by comparing our results to v_2 data. Actually, extraction of transport coefficients by matching the output of hydrodynamic and/or kinetic simulations to data is not at all straightforward, as discussed e.g. in Refs. [9, 48–50]. In particular, to extract η/s from v_2 measurements, a possible route is to first constrain initial T_i and final T_f temperatures (that are used to run the coupled set of hydro-chiral equations) by matching calculated spectra to data and, afterwards, extract η/s from v_2 data – see e.g. Refs. [48, 51]. In addition, although we use a semi-realistic initial condition (we use a Glauber smooth initial condition), a fluctuating, lumpy initial condition leads to lower elliptic flow along with other interesting effects [52–54] that certainly have an impact on the extraction of transport coefficients.

The paper is organized as follows. In Section II we describe the coupling of the chiral fields to the 2 + 1 hydrodynamic model. In Section III we describe the initial conditions and the freeze-out prescription used in the simulations. We then show and discuss our results in Section IV, and conclude in Section V. In Appendix A we briefly overview the LSM and the calculation of the speed of sound and of the shear viscosity from the linearized Boltzmann equation in the relaxation time approximation. In Appendix B we discuss the dependence of our results on the cut-off that we must impose on the value of η/s due to the breakdown of viscous hydrodynamics when nonequilibrium effects start to dominate.

II. COUPLED CHIRAL-HYDRO DYNAMICS

In this section we describe the model of coupling chiral fields to hydrodynamical variables. The evolution of the chiral fields is described by the LSM [35] and hydrodynamics is described by dissipative hydrodynamic equations [32–34]. This hydrodynamic formalism goes beyond the well-known Israel–Stewart theory [55–57] in that it includes all second-order terms in velocity gradients that can appear in the stress–energy tensor of a conformal fluid – see e.g. Ref. [58]. This hydro model has been applied to model the expansion of the QGP in Refs. [48] and [51].

In order to set notation and make the paper self-contained, we start with the LSM model. The Lagrangian density of the model, given in terms of quark $q = (u, d)$ and chiral $\phi_a = (\sigma, \vec{\pi})$ fields, is written as (we use the signature for the metric $g_{\mu\nu} = (+, -, -, -)$)

$$\mathcal{L} = \mathcal{L}_q + \mathcal{L}_\phi, \quad (1)$$

with

$$\mathcal{L}_q = \bar{q} [i\gamma^\mu \partial_\mu - g(\sigma + \gamma_5 \vec{\tau} \cdot \vec{\pi})] q, \quad (2)$$

and

$$\mathcal{L}_\phi = \frac{1}{2} (\partial_\mu \sigma \partial^\mu \sigma + \partial_\mu \vec{\pi} \cdot \partial^\mu \vec{\pi}) - U(\sigma, \vec{\pi}). \quad (3)$$

where

$$\begin{aligned} U(\sigma, \vec{\pi}) &\equiv U(\phi) = \frac{\lambda^2}{4} \phi^2 - h_q \sigma - U_0 \\ &= \frac{\lambda^2}{4} (\sigma^2 + \pi^2 - v^2)^2 - h_q \sigma - U_0, \end{aligned} \quad (4)$$

is the potential which exhibits chiral symmetry breaking – with $\phi^2 = \sigma^2 + \pi^2$. At the level of approximation we work in the present paper, parameters are fixed as follows. The vacuum expectation values of the condensates are taken $\langle \sigma \rangle = f_\pi$ and $\langle \vec{\pi} \rangle = 0$, with the pion decay constant $f_\pi = 93$ MeV. Also, the partially conserved axial–vector current relation yields $h_q = f_\pi m_\pi^2$ with $m_\pi = 138$ MeV. This leads to $v^2 = f_\pi^2 - m_\pi^2/\lambda^2$. A mass $m_\sigma = \sqrt{2\lambda^2 f_\pi^2 + m_\pi^2} \sim 600$ MeV is obtained if $\lambda^2 = 20$. The constant U_0 is chosen such that the potential energy vanishes in the ground state.

Following Paech et al. [41, 42], we split the energy-momentum tensor as

$$T^{\mu\nu} = T_q^{\mu\nu} + T_\phi^{\mu\nu}. \quad (5)$$

As mentioned previously, the quarks and antiquarks are assumed to constitute a heat bath in local thermal equilibrium and their dynamical evolution will be determined by viscous relativistic hydrodynamics, so that:

$$T_q^{\mu\nu} = (\epsilon + p)u^\mu u^\nu - pg^{\mu\nu} + \Pi^{\mu\nu}, \quad (6)$$

where u_μ is the four-velocity normalized as $u_\mu u^\mu = 1$, $\Pi^{\mu\nu}$ is the viscous shear-tensor, and $\epsilon = \epsilon(\phi, T)$ and

$p = p(\phi, T)$ are the energy density and pressure (by definition) at equilibrium at local temperature T – their explicit expressions are given in Appendix A. The contribution from the chiral fields to the energy-momentum tensor is given by

$$T_\phi^{\mu\nu} = \sum_{a=0}^4 \frac{\partial \langle \mathcal{L}_\phi \rangle}{\partial (\partial_\mu \phi_a)} \partial^\nu \phi_a - g^{\mu\nu} \langle \mathcal{L}_\phi \rangle, \quad (7)$$

where $\langle \dots \rangle$ means local thermal average.

The hydrodynamic equations of motion are obtained from conservation of the energy-momentum tensor, $D_\mu T^{\mu\nu} = 0$, where D_μ is the geometric covariant derivative. We employ Milne coordinates (appropriate for a $(2+1)$ flow dynamics) defined by proper time $\tau = \sqrt{t^2 - z^2}$ and rapidity $\psi = \text{arctanh}(z/t)$. The hydrodynamic velocity is $u = (u^\tau, u^x, u^y, 0)$ and the metric tensor reads $g_{\mu\nu} = (-1, 1, 1, \tau^2)$. In the transverse plane we use Cartesian coordinates $x^i = (x, y)$, so that the only non-vanishing Christoffel symbols are $\Gamma_{\psi\psi}^\tau = \tau$ and $\Gamma_{\tau\psi}^\psi = 1/\tau$. Since we assume boost-invariance all quantities are independent of rapidity. The conservation equations then read

$$\begin{aligned} D\epsilon &= -(\epsilon + p)\nabla_\mu u^\mu + \Pi^{\mu\nu}\sigma_{\mu\nu} \\ &\quad + g(\rho_s D\sigma + \vec{\rho}_{ps} \cdot D\vec{\pi}), \end{aligned} \quad (8)$$

$$\begin{aligned} (\epsilon + p)Du^i &= c_s^2(g^{ij}\partial_j\epsilon - u^i u^\alpha \partial_\alpha \epsilon) - \Delta_\alpha^i D_\beta \Pi^{\alpha\beta} \\ &\quad + g(\rho_s \nabla^i \sigma + \vec{\rho}_{ps} \cdot \nabla^i \vec{\pi}), \end{aligned} \quad (9)$$

where $\Delta^{\mu\nu} = g^{\mu\nu} - u^\mu u^\nu$ is a projector (orthogonal to the fluid velocity), c_s is the speed of sound, and $\rho_s = \langle \bar{q}q \rangle$ and $\vec{\rho}_{ps} = \langle \bar{q}\gamma_5 \vec{\tau}q \rangle$ are the local thermal averages of the scalar and pseudo-vector chiral densities – their explicit expressions are given in Appendix A. It is seen that the chiral densities act as sources for the evolution of the hydrodynamic variables ϵ and u^μ . Here, $D = u_\mu D^\mu$ is the comoving time derivative, $\nabla_\mu = \Delta_{\mu\alpha} D^\alpha$ is the spatial gradient, $\sigma_{\mu\nu}$ is the shear tensor:

$$\sigma^{\mu\nu} = \nabla^{(\mu} u^{\nu)}. \quad (10)$$

The angular braces around Lorentz indices denotes the spatial, symmetric and traceless part of a tensor, i.e. if $A^{\mu\nu}$ is a tensor then $A^{(\mu\nu)}$ means:

$$A^{(\mu\nu)} = \frac{1}{2} \left(\Delta^{\mu\alpha} \Delta^{\nu\gamma} + \Delta^{\mu\gamma} \Delta^{\alpha\nu} - \frac{2}{3} \Delta^{\mu\nu} \Delta^{\alpha\gamma} \right) A_{\alpha\gamma}. \quad (11)$$

The evolution of the shear tensor depends only indirectly on the chiral fields and it is given by

$$\begin{aligned} \partial_\tau \Pi^{i\alpha} &= -\frac{4}{3u^\tau} \Pi^{i\alpha} \nabla_\mu u^\mu - \frac{1}{\tau_\pi u^\tau} \Pi^{i\alpha} + \frac{\eta}{\tau_\pi u^\tau} \sigma^{i\alpha} \\ &\quad - \frac{\lambda_1}{2\tau_\pi \eta^2 u^\tau} \Pi_\mu^{<i} \Pi^{\alpha>\mu} - \frac{u^i \Pi_\mu^\alpha + u^\alpha \Pi_\mu^i}{u^\tau} D u^\mu \\ &\quad - \frac{u^j}{u^\tau} \partial_j \Pi^{i\alpha}, \end{aligned} \quad (12)$$

where η is the shear viscosity and (τ_π, λ_1) are second-order transport coefficients. We note that Israel–Stewart formalism is recovered from these equations when $\lambda_1 = 0$.

In the Milne coordinates, the classical equations of motion for the chiral fields evolving in the background of the quark fluid read

$$\left(\partial_\tau^2 + \frac{1}{\tau}\partial_\tau - \partial_i^2\right)\sigma + \frac{\delta U}{\delta\sigma} = -g\rho_s, \quad (13)$$

$$\left(\partial_\tau^2 + \frac{1}{\tau}\partial_\tau - \partial_i^2\right)\vec{\pi} + \frac{\delta U}{\delta\vec{\pi}} = -g\vec{\rho}_{ps}, \quad (14)$$

where ρ_s and $\vec{\rho}_{ps}$ are the scalar and pseudo-scalar chiral condensates defined above.

In this way, the evolution of the chiral fields affects the evolution of the quark fluid through the sources in the energy–momentum conservation equations; in turn, the quark fluid affects the evolution of the chiral fields through the densities ρ_s and $\vec{\rho}_{ps}$.

III. SOLVING THE EQUATIONS

We solve the hydrodynamic equations given in Eqs. (8) and (9) using the publicly available code of Luzum and Romatschke [48]. We need to supply the locally temperature-dependent transport coefficients η , τ_π and λ_1 , and speed of sound c_s . In addition, we need to specify initial conditions for the energy density ϵ , velocities u_1 and u_2 , and the components of the shear tensor. To solve the equations of motion for the chiral fields, Eqs. (13) and (14), we use a simple finite-difference scheme both in the proper-time and space variables. Here also, one needs to provide initial conditions for the fields and their derivatives.

In all calculations performed in the present paper, we use a $13 \text{ fm} \times 13 \text{ fm}$ transverse plane. In the next subsections we discuss the values used for the input constants and initial conditions.

A. Transport coefficients and the speed of sound

As a prototypical example of a relativistic fluid, we will use $\tau_\pi = 2(2 - \ln 2)\eta/sT$ and $\lambda_1 = \eta/2\pi T$, that correspond – in a gradient expansion at second-order – to a supersymmetric Super–Yang–Mills plasma [32–34]. However, as mentioned in the Introduction, we will not use $c_s^2 = 1/3$ and $\eta/s = 1/4\pi$ appropriate to the Super–Yang–Mills plasma. The temperature dependence of the speed of sound is obtained within the LSM and that of η is obtained using the linearized Boltzmann equation in the relaxation time approximation within the chiral model of Ref. [28]. We discuss these in the Appendix A.

We note that the value that we use for the relaxation time $\tau_\pi = 2(2 - \ln 2)\eta/sT$ is not the exact value of the Super–Yang–Mills plasma [59, 60]. Rather, it is the

value obtained through a second-order gradient expansion, that is equivalent to a Taylor expansion of the retarded Green’s function that linearly relates a dissipative current and a thermodynamical force. The expression for τ_π derived in this way is in general different from the one obtained directly from the first pole of the retarded Green’s function. Moreover, as shown in Refs. [59, 60], the true dynamics of the long-wavelength and low frequency modes of strongly coupled theories is not generally described by relaxation-type equations, i.e., the evolution equation for the shear tensor includes terms with second time derivatives of the thermodynamic forces – see also Ref. [61].

In this connection, it is important to remark that it was shown in previous hydrodynamic simulations (without chiral fields) [48, 51] that, for values of $\eta/s \lesssim 0.2$, the results for the hadronic observables do not depend strongly on the choices for the second-order transport coefficients, provided that $\lambda_1 \neq 0$. The influence of terms with second time derivatives of the thermodynamic forces in the evolution of the shear tensor of the QGP is still an open issue that surely deserves further investigation. In this work we will neglect such terms and use instead the relaxation-type equation given in Eq. (12), that is obtained from a second-order gradient expansion.

B. Initial conditions

For the initial transverse velocity and shear tensor we use $u^x = u^y = 0$, which implies vanishing initial vorticity, and $(\Pi^{xx}, \Pi^{xy}, \Pi^{yy}) = 0$. The initialization time is set to $\tau_0 = 1 \text{ fm}/c$. It has been shown before that the evolution of the shear tensor $\Pi^{\mu\nu}$ is quite insensitive to the initialization values, the difference being appreciable only at very early times (see e.g. Ref. [50]). We have verified that the elliptic flow shows very little sensitivity to the initialization of the shear tensor as well. The initial temperature at the center of the fireball is set to $T_i = 333 \text{ MeV}$. This value for T_i has been used in previous hydrodynamic simulations and leads to kaon multiplicity and $\langle p_T \rangle$ that are in good agreement with RHIC data [48, 51].

The initial energy density profile is calculated using Glauber’s model, in which for a given impact parameter b we have

$$\epsilon(\tau_0, x, y, b) = C \sigma T_A(x + b/2, y) T_A(x - b/2, y), \quad (15)$$

where C is a constant chosen such that $\epsilon(\tau_0, 0, 0, 0)$ corresponds to a given initialization temperature T_0 via the EOS, the cross-section σ is taken to be $\sigma = 40 \text{ mb}$, and T_A is the nuclear thickness function given by

$$T_A(x, y) = \int_{-\infty}^{\infty} \delta_A(x, y, z) dz, \quad (16)$$

with δ_A is the density distribution for the gold nucleus,

taken to be of a Woods-Saxon form

$$\delta_A(x, y, z) = \frac{\delta_0}{1 + \exp[(|\vec{x}| - R_0)/\chi]}, \quad (17)$$

where $\vec{x} = (x, y, z)$, $R_0 = 6.4$ fm and $\chi = 0.54$ fm. The parameter δ_0 is chosen such that $\int d^3\mathbf{x} \delta_A(\mathbf{x}) = 197$, as appropriate for Au nuclei.

As a reasonable ansatz for the initial condition of the chiral fields we use

$$\vec{\pi}(\tau_0, \vec{r}) = 0 \quad \text{and} \quad \sigma(\tau_0, \vec{r}) = f_\pi \left[1 - e^{-(r/r_0)^2} \right], \quad (18)$$

with $r^2 = x^2 + y^2$ and $r_0 = 9$ fm. In this way, the chiral condensate nearly vanishes at the center where the temperature of the fluid is larger and interpolates to f_π where the temperature is lower.

C. Freeze-out scheme

In our simulations we use the isothermal Cooper-Frye freeze-out prescription [62] in which the conversion from hydrodynamic to particle degrees of freedom takes place in a three-dimensional hypersurface. The spectrum for a single on-shell particle with momentum $p^\mu = (E, \vec{p})$ and degeneracy d is

$$E \frac{dN}{d^3p} = \frac{d}{(2\pi)^3} \int p_\mu d\Sigma^\mu f(x^\mu, p^\mu), \quad (19)$$

where $d\Sigma^\mu$ is the normal vector on the hypersurface. The non-equilibrium distribution function f is given by Grad's quadratic ansatz [63]:

$$\begin{aligned} f(x^\mu, p^\mu) &= f_0(x^\mu, p^\mu) \\ &+ f_0(x^\mu, p^\mu) [1 \mp f_0(x^\mu, p^\mu)] \frac{p_\mu p_\nu \Pi^{\mu\nu}}{2T^2(p + \epsilon)} \\ &\simeq \left[1 + \frac{p_\mu p_\nu \Pi^{\mu\nu}}{2T^2(p + \epsilon)} \right] \exp\left(\frac{-p_\mu u^\mu}{T}\right), \quad (20) \end{aligned}$$

where f_0 is the Fermi-Dirac distribution. The approximation in the third line holds when $p \gg T$, and it is used in our simulations. The systematic error of this approximation is very small at low transverse momentum $p_T \lesssim 2.5$ GeV, so we do not expect our results to have a significant error coming from this approximation (see Ref. [48]).

We calculate the spectra for particle resonances with masses up to 2 GeV and then determine the spectra of stable particles including feed-down contributions. For this last step we use the AZHYDRO package [64–66]. In the present paper we will focus on the elliptic flow coefficient v_2 and also on v_4 at central rapidity, which are related to the particle spectra (including feed-down contributions) by

$$E \frac{dN}{d^3p} = v_0(p_T, b) \left[1 + \sum_{n=1}^{\infty} 2v_n(p_T, b) \cos(n\varphi) \right], \quad (21)$$

with $\varphi = \arctan(p_y/p_x)$ and $p_T = (p_x^2 + p_y^2)^{1/2}$. For the freeze-out temperature we take $T_f = 130$ MeV. This value for T_f is slightly smaller than the one usually employed in viscous hydrodynamic simulations of Au+Au collisions of $T_f \sim 140$ MeV, but allows us to study a broader range of temperatures near our value of T_c in order to determine the influence of chiral fields dynamics on hadronic observables.

IV. RESULTS

We now go over to discuss our results. We start with a very important input to the hydro equations, the square of the speed of sound $c_s^2 = dp/d\epsilon$. In Fig. 1 we show c_s^2 as predicted by the LSM – its explicit expression is given in Appendix A – for three values of the coupling constant, namely $g = 3.0, 3.2, 3.4$, which correspond to a smooth crossover. The reason to consider these values for g is that recent works have shown that the crossover phase transition without a thermodynamic region where the sound velocity drops to zero leads to a faster time development of the system and helps to reproduce RHIC data with hydrodynamic simulations [67–69]. Moreover, Lattice QCD calculations also favor a smooth crossover with a relatively soft dip in c_s^2 over a first-order phase transition (see e.g. Refs. [70–74]). In our case, the first-order transition is obtained when $g = 3.8$. As it can be seen from Fig. 1, lowering the value of g leads to a softening of the crossover and a raise in the critical temperature T_c . For large temperatures the conformal limit $c_s^2 = 1/3$ is reached, while for low values c_s^2 goes to zero. For $g \sim 3.2$ the behavior of c_s^2 with temperature is in qualitative agreement with that obtained in Lattice QCD calculations [70–74] and with that favored by hydrodynamic simulations based on different interpolation schemes used to join Lattice QCD and hadron resonance gas equations of state (see e.g. Refs. [67–69]). For $g > 3.4$ or $g < 3$, the dip in c_s^2 at T_c becomes very sharp or fades away, respectively, resulting in a temperature dependence that is in disagreement with the one obtained in Lattice QCD calculations.

The critical temperature for these values of the LSM parameters is $T_c \sim 150$ MeV, which is smaller than the value ~ 170 MeV obtained from Lattice QCD simulations [70–74]. Within the LSM it is not possible to obtain much larger values for T_c without going to very low values of g . These lower values of g correspond to a very soft crossover with an almost inappreciable drop in c_s^2 that is not in agreement with the results the Lattice QCD. The relatively low value for T_c used here does not constitute a serious limitation to our aim of obtaining a qualitative understanding of the impact of the evolution of the chiral fields on hadronic observables, since we expect the trends obtained in this paper to hold in more realistic scenarios.

Another input to the hydrodynamic simulation is the

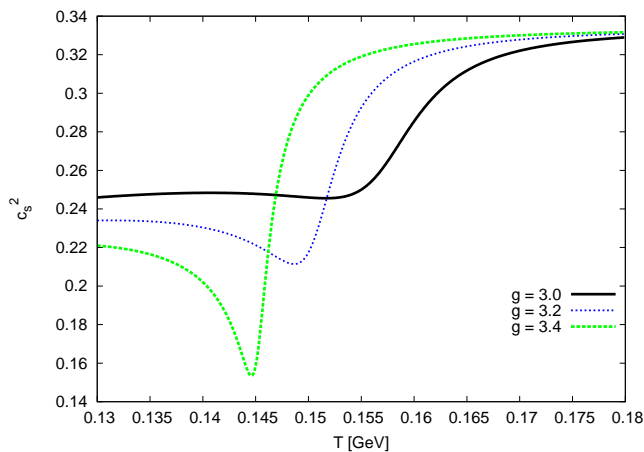


FIG. 1: (Color online) Square of the sound speed c_s^2 of the LSM as a function of temperature, for three values of the chiral coupling: $g = 3, 3.2, 3.4$.

ratio η/s as a function of temperature, which we calculate in the LSM from the linearized Boltzmann equation in the relaxation time approximation (details are given in Appendix A). Fig. 2 shows η/s as a function of temperature in a region close to T_c , for $g = 3, 3.2, 3.4$. It is seen that η/s decreases significantly when approaching T_c from below, and remains almost constant and rather small at $T > T_c$. This behavior is qualitatively similar to that found in other approaches such as the Boltzmann–hydrodynamics hybrid approach [75], the NJL model [28] and Chiral Perturbation Theory [76], although, as already indicated, the value of T_c obtained here is smaller. It is also seen that when the value of g increases the variation of η/s with temperature is more abrupt, decreasing faster at $T < T_c$ and thus remaining small for a larger range of temperatures.

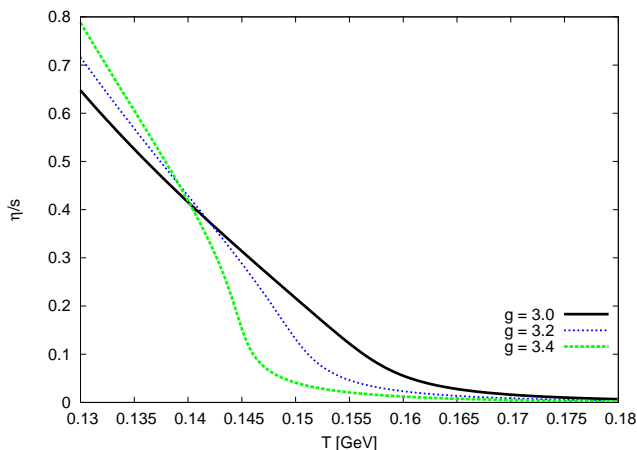


FIG. 2: (Color online) η/s of the LSM as a function of temperature, for three values of the chiral coupling: $g = 3, 3.2, 3.4$.

At this stage it is appropriate to note an important point concerning the rise of η/s with decreasing tem-

perature in the low temperature stage. By construction, any hydrodynamic description of matter necessarily breaks down when the viscosity is large enough that nonequilibrium effects are as important, or even more important than the equilibrium ones. For example in the context of Grad’s quadratic ansatz that is usually employed at freeze-out, this occurs when the nonequilibrium correction to the distribution function is comparable – or exceeds – the equilibrium one. In the context of relativistic heavy-ion collisions numerous hydrodynamic simulations (usually with *temperature-independent* η/s) have shown that *large enough* means $\eta/s \sim 0.3 - 0.5$ [10, 13, 50, 75, 77–80]. For larger values of η/s it is not possible to match the predictions of hydrodynamic models to RHIC data. Moreover, it has been shown by direct comparison to results obtained with Boltzmann equation that for matter created at RHIC, viscous hydrodynamics fails to reproduce the results of Boltzmann equation if $\eta/s \gtrsim 0.2$ [81]. Beyond this value, an appropriate treatment of the dynamics of this matter should switch smoothly from a viscous hydrodynamic description to a kinetic one, in which the issue of breakdown due to large viscosity (i.e. dissipation) does not arise. For recent developments and applications of this hybrid description see Refs. [10, 75].

Since the model used here is purely hydrodynamic, a cut-off for the value of η/s must be *imposed* in order to avoid the breakdown of the fluid description. The value of η/s at which it is sensible to impose this cut-off is constrained by the comparison of results obtained from hydrodynamic and kinetic simulations to data. For this reason, in our simulations we set $\eta/s \leq 0.4$, which corresponds to $T \sim 140$ MeV for the three values of the chiral coupling, namely $g = 3, 3.2, 3.4$, the values we consider in the present paper. We emphasize that in all of our simulations with $g = 3, 3.2, 3.4$ the *average* value of η/s throughout the hydrodynamic evolution is ~ 0.11 , and thus it remains well below the value at which viscous hydrodynamics breaks down ($\eta/s \sim 0.3 - 0.5$).

In Appendix B we analyse the dependence of our results on the choice of different cut-off values for η/s . We find that, although the values of v_2 and $v_4/(v_2)^2$ do change, the differences between the cases including or not the chiral fields as sources remain essentially the same, and thus our main conclusions are not sensitive to the value imposed for the cut-off.

Knowing c_s^2 and η/s as functions of the temperature, we can now go over to discuss the momentum anisotropies obtained from the simulations. Fig. 3 shows the charged-hadron elliptic flow v_2 calculated with either the temperature-dependent η/s of the LSM or a temperature-independent $\eta/s = 0.11$, which corresponds to the average of η/s throughout the hydrodynamic evolution over the temperature interval from T_i to T_f . In both cases, we set $g = 3.2$ and compare the results obtained by taking or not taking into account the source terms in the hydrodynamic equations.

It is seen from Fig. 3 that both for a temperature-

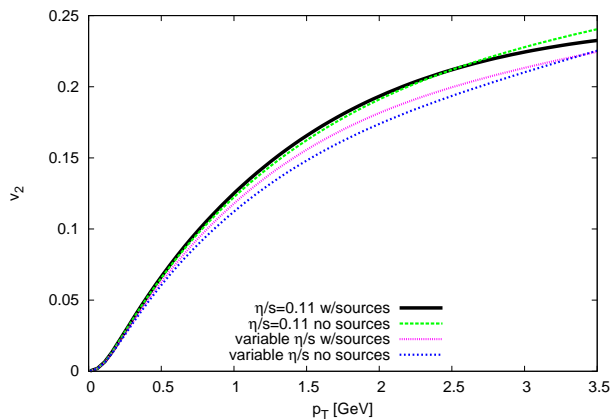


FIG. 3: (Color online) Elliptic flow of charged-hadrons calculated taking or not taking into account the source terms in the hydrodynamic equations, for either a temperature-dependent or a temperature-independent η/s which is the averaged value throughout the evolution of the fireball. The value of the coupling constant is $g = 3.2$.

dependent and a temperature-independent η/s , the elliptic flow does not depend strongly on the chiral sources. For a temperature-independent η/s , v_2 turns out to be practically independent of the dynamics of the chiral sources for $p_T < 3$ GeV. In contrast, for the temperature-dependent η/s there are small, but visible differences in the elliptic flow calculated with or without the chiral sources. Specifically, v_2 is slightly larger and reaches a maximum at $p_T \sim 2$ GeV when the chiral fields are taken into account as sources for the hydrodynamic variables.

Comparing the behavior of v_2 for temperature-independent or temperature-dependent η/s , it is seen that a temperature-dependent η/s leads to a smaller elliptic flow. This fact has already been seen in the studies of Refs. [8, 9, 11] by performing hydrodynamic simulations (not coupled to chiral fields) with different parameterizations for temperature-dependent η/s (usually a step-function dependence or some slight variation), and in Ref. [75] from a Boltzmann-hydrodynamics hybrid approach. See also Refs. [10, 12] for related studies. In particular, it was found in Ref. [8] that v_2 at Au+Au collisions at the largest RHIC energy is dominated by the shear viscosity in the hadronic phase and largely insensitive to the viscosity of the QGP. A similar conclusion was reached in Refs. [9, 11]. It is interesting to note that, according to recent viscous hydrodynamic simulations with temperature dependent η/s , at LHC energies the situation is exactly the opposite, i.e. the elliptic flow becomes sensitive to the QGP viscosity and insensitive to the hadronic viscosity [8, 9]. As noted in Ref. [9], the fact v_2 depends rather weakly on the temperature dependence of η/s poses serious challenges to the precise extraction of this ratio from this hadronic observable. For this reason, and also due to the uncertainty in the ini-

tial conditions in heavy-ion collisions at RHIC and LHC, it has now become important to calculate higher-order Fourier moments v_3, \dots in viscous hydrodynamic simulations, which may provide further crucial constraints on η/s and on models used to calculate QGP initial conditions – see e.g. Refs. [75, 82–87].

Returning to our results in Fig. 3, it seems clear the difficulties in extracting (an average value of) η/s from data on v_2 . The results show that uncertainties associated with the dependence of η/s on temperature lead to appreciable changes in the curve of v_2 versus p_T . Such an uncertainty should be added to the theoretical uncertainty that comes e.g. from the initial conditions (for example using Color Glass Condensate or Glauber initial conditions), the freeze-out process (as issues concerning Grad’s quadratic ansatz), as well as from other sources, that according to recent studies add up to an overall uncertainty which can be roughly estimated in 0.1 [48, 51].

As mentioned in the Introduction, the fact that v_2 depends somewhat on the evolution of the chiral fields in the case of a temperature-dependent η/s has already been seen in the study by Plumari et al [47] within Boltzmann-Vlasov simulations on the NJL model. Our results show that this also happens in a purely hydrodynamic simulation as well.

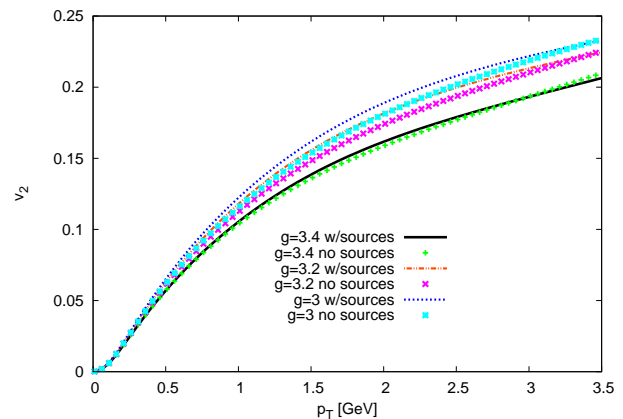


FIG. 4: (Color online) Elliptic flow of charged-hadrons calculated taking or not taking into account the source terms in the hydrodynamic equations, for $g = 3, 3.2, 3.4$ and a temperature-dependent η/s .

Since our approach is phenomenological, it is important to determine the sensitivity of our conclusions regarding the influence of the chiral fields on v_2 to the value of the coupling constant g . Fig. 4 shows the elliptic flow of charged-hadrons calculated taking or not taking into account the source terms in the hydrodynamic equations, for $g = 3, 3.2, 3.4$ and a temperature-dependent η/s . It is seen that when the value of g increases, v_2 decreases. This is due to the fact that for larger values of g , c_s^2 near the transition region becomes smaller which means that pressure gradients are converted into flow less efficiently, thus resulting in lower values of v_2 . The difference in the

values of v_2 calculated including or not the chiral fields as sources is seen to become smaller with increasing g , which supports the conclusion reached earlier that the influence of the chiral fields on v_2 is rather small.

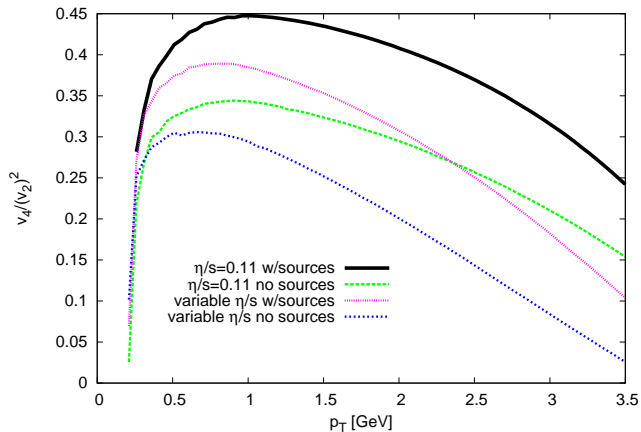


FIG. 5: (Color online) $v_4/(v_2)^2$ for charged-hadrons calculated taking or not taking into account the chiral fields as sources for the hydrodynamic equations, for either a temperature-dependent or a temperature-independent η/s . The value of the coupling constant is $g = 3.2$.

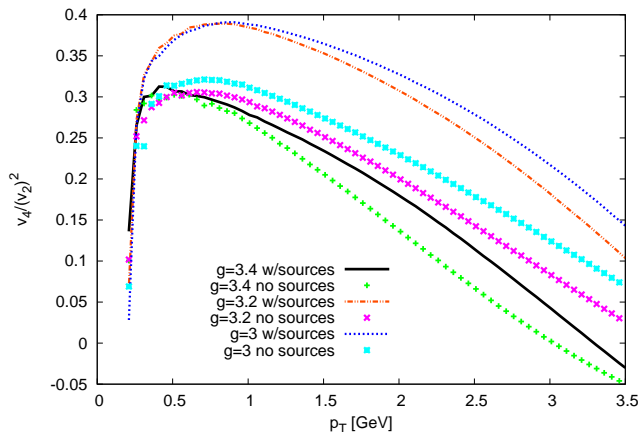


FIG. 6: (Color online) $v_4/(v_2)^2$ for charged-hadrons calculated taking or not taking into account the chiral fields as sources for the hydrodynamic equations, for $g = 3, 3.2, 3.4$ and a temperature-dependent η/s .

Another interesting observable to analyse is $v_4/(v_2)^2$, which has only recently been theoretically investigated. See in particular Refs. [88, 89] for a detailed account of the physics (and caveats – see below) involved in this observable within dissipative hydrodynamics. See also Ref. [47] for a calculation of $v_4/(v_2)^2$ within Boltzmann–Vlasov formalism. Fig. 5 shows $v_4/(v_2)^2$ for the same cases as in Fig. 3. In contrast to what happens with v_2 , it is seen that $v_4/(v_2)^2$ is significantly affected by the dynamics of the chiral fields even at low transverse

momentum and for a temperature-independent η/s . In particular, the values of $v_4/(v_2)^2$ are larger when the chiral fields are included as sources in the hydrodynamic equations, and the behavior with p_T is somewhat different too. It is also seen that a temperature-independent η/s leads to larger $v_4/(v_2)^2$.

At this point, a comment on the possible extraction of η/s from $v_4/(v_2)^2$ data by matching to hydrodynamic simulations is in order. It is known that the dependence of $v_4/(v_2)^2$ on transverse momentum that is obtained from viscous hydrodynamics does not agree with the almost constant value of $v_4/(v_2)^2 \sim 1$ measured at RHIC (see Refs. [88, 89]). Ideal hydrodynamics predicts $v_4/(v_2)^2 = 0.5$, but quite surprisingly viscous hydrodynamics yields a strongly dependent ratio, as shown, for example, in Fig. 5. A possible explanation for this discrepancy has been put forward by Luzum and Ollitrault [88, 89], who realized that Grad’s quadratic ansatz for the nonequilibrium correction δf to the particle distribution function may not be valid for the freeze-out process in heavy-ion collisions. See also Refs. [90–93] for recent work on the reliability of Grad’s ansatz. By performing viscous hydrodynamic simulations with different dependencies of δf on p_T , the authors of Refs. [88, 89] have found that RHIC data on $v_4/(v_2)^2$ favors a momentum dependence between linear and quadratic. In spite of this, we have chosen to show results on $v_4/(v_2)^2$ to emphasize that, although the values for this observable are very different from those measured at RHIC (because we are using Grad’s quadratic ansatz at freeze-out), they are much more sensitive than v_2 to the evolution of the chiral fields. We expect this feature of $v_4/(v_2)^2$ to hold when other forms for δf are used in the simulations, although further work is needed to confirm this expectation.

As with v_2 , it is important to determine the dependence of our results and conclusions on the value of g . Fig. 6 shows $v_4/(v_2)^2$ calculated including or not the sources in the hydrodynamic equations, for $g = 3, 3.2, 3.4$ and a temperature-dependent η/s . It is seen that the difference in the values of $v_4/(v_2)^2$ calculated including or not the chiral fields as sources becomes smaller with increasing g , but is still relatively large at $g = 3.4$. Moreover, it is seen that the behavior of this ratio with p_T does not depend strongly on the value of g . These results obtained with different values of g support the conclusion mentioned before that $v_4/(v_2)^2$ is more sensitive than v_2 to the influence of the chiral fields on the evolution of the quark fluid.

V. CONCLUSIONS

We have studied the evolution of the fireball created at RHIC within second-order viscous hydrodynamics coupled self-consistently to the LSM, focusing on the impact of the dynamics of the chiral fields on the hadronic observables v_2 and $v_4/(v_2)^2$. We have compared the results obtained when the chiral fields are included or not as

sources in the hydrodynamic equations. The comparisons were made using both temperature-independent and temperature-dependent η/s . The temperature dependence of η/s was calculated in the LSM using the linearized Boltzmann equation.

We have found that the values of v_2 do not depend strongly on the evolution of the chiral fields. Specifically, for a temperature-independent η/s this dependence is negligible for $p_T < 3$ GeV, while for a temperature-dependent η/s it is appreciable but still small even at small p_T . We have also found that the ratio $v_4/(v_2)^2$ is much more sensitive to the dynamics of the chiral fields, being larger when these fields are taken into account as sources in the hydrodynamic equations, in both situations of the temperature dependence of η/s .

In line with the results of Refs. [8–10], our results show that not knowing precisely the temperature-dependence of η/s leads to further uncertainties in attempts of extracting this ratio from data on v_2 , in addition to the uncertainties that stem from the initial conditions and the freeze-out process, among others sources. It is worth noting that despite the coupling of chiral sources to the hydrodynamic evolution would add further uncertainties, they are not very big.

The model used in this work leaves room for improvements in different directions. Probably, the most important ones for our analysis are including bulk viscosity in the hydrodynamic equations and fluctuations of the chiral fields. This latter effect would act as noise sources in the classical equations of motion. We believe that the qualitative trends and the general conclusions extracted from our results will hold when these effects are taken into account. Work is in progress where these two aspects are taken into account in a viscous hydrodynamic simulation and their impact on observables will be reported in a forthcoming publication.

Appendix A: Linear σ model

In this Appendix we will briefly review the relevant aspects of linear σ model for the present paper, as well as the calculation of η from the linearized Boltzmann equation in the relaxation time approximation.

As mentioned before, as an effective theory of the chiral symmetry breaking dynamics we consider the linear σ model coupled to two flavors of constitutive quarks. The Lagrangian density of the coupled system is given in Eq. (1). The quark fluid is considered as a thermal bath for the chiral field, and therefore it can be integrated out to obtain the effective potential V_e for the chiral fields in the presence of that bath of quarks. In order to calculate the equilibrium pressure density $p(\phi, T) = -V_e(\phi, T) + U(\phi)$, we use the one-loop effective potential [41, 42]:

$$V_e(\phi, T) = U(\phi) - d_q T \int \frac{d^3 p}{(2\pi)^3} \ln \left(1 + e^{-E/T} \right), \quad (\text{A1})$$

where $d_q = 24$ is the color-spin-isospin-baryon charge degeneracy of the quarks and the energy $E = (p^2 + m_q^2)^{1/2}$ with $m_q^2 = g^2 \phi^2$. The equilibrium energy density is just

$$\epsilon(\phi, T) = d_q \int \frac{d^3 p}{(2\pi)^3} f_0 E. \quad (\text{A2})$$

From p and ϵ , the square of the speed of sound and the entropy density follow: $c_s^2 = dp/d\epsilon$ and $s = \partial p/\partial T$.

The local thermal averages of the scalar and pseudo-vector chiral densities $\rho_s = \langle \bar{q}q \rangle$ and $\vec{\rho}_{ps} = \langle \bar{q}\gamma_5 \vec{\tau}q \rangle$ enter as sources in the hydrodynamic equations. Explicitly, they are given by:

$$\rho_s = g\sigma d_q \int \frac{d^3 p}{(2\pi)^3} \frac{1}{E} f_0, \quad (\text{A3})$$

$$\vec{\rho}_{ps} = g\vec{\pi} d_q \int \frac{d^3 p}{(2\pi)^3} \frac{1}{E} f_0. \quad (\text{A4})$$

The LSM exhibits a first-order phase transition, a crossover and a critical end point, depending on the value of the chiral coupling constant g . The crossover phase transition is not a genuine phase transition since all thermodynamic functions change smoothly with temperature. However, such changes may be quite sudden in a narrow temperature range. As indicated in Section IV, throughout this work we set $g = 3$, $g = 3.2$ and $g = 3.4$, which correspond to a smooth crossover and lead to a temperature-dependent sound speed that resembles that of Lattice QCD.

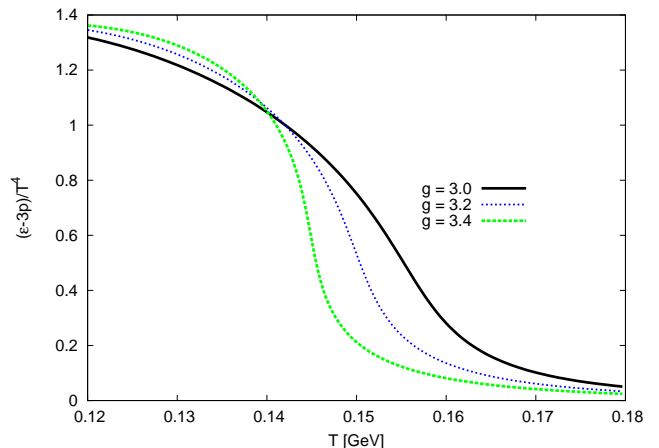


FIG. 7: (Color online) $(\epsilon - 3p)/T^4$ of the LSM as a function of temperature for $g = 3, 3.2, 3.4$.

Here we model the expansion of the QGP using viscous hydrodynamics with the bulk viscosity ζ set to zero. It is known that ζ scales as $c_s^2 - 1/3$, so from Fig. 1 it is clear that for the LSM $\zeta \neq 0$ (see also Refs. [28, 29]). Recent Lattice QCD results indicate that the quark-gluon matter EOS departures from the conformal description [70–74], although it is common practice to neglect ζ in the hydrodynamic equations while using an EOS inspired on Lattice QCD. An estimate for the temperature-dependence

and the relative importance of ζ can be obtained from $(\epsilon - 3p)/T^4$, which measures the deviation from the conformal limit. Fig. 7 shows this quantity calculated in the LSM as a function of temperature, for $g = 3, 3.2, 3.4$. It is seen that, for the range of temperatures of interest $T \geq 130$ MeV, $(\epsilon - 3p)/T^4$ is small except at $T \leq T_c$ where it rises abruptly reaching significant values. The increase in $(\epsilon - 3p)/T^4$ near T_c is sharper for larger values of g . It has been shown before that the hydrodynamic evolution is affected by bulk viscosity, for example reducing the elliptic flow, inducing the phenomenon of cavitation or modifying the freeze-out process [13, 79, 80]. Although it is reasonable to assume that these changes will not affect in a dramatic way the differences in v_2 and $v_4/(v_2)^2$ that result from including or not the chiral fields as sources for the evolution of the quark fluid, a more thorough investigation of this particular issue is necessary.

We now go over to the calculation of the shear viscosity. In order to calculate η we adopt the results of Ref [28], which are based on the linearized Boltzmann equation in the relaxation time approximation. In the relaxation time approximation the shear viscosity is given by

$$\eta = \frac{4\tau}{5T} \int \frac{d^3p}{(2\pi)^3} \frac{p^4}{E^2} f_0(1 - f_0) \quad (\text{A5})$$

where $\tau = \tau(T)$ is the collision time. $\tau(T)$ is calculated from the averaged cross sections $\bar{\sigma}$ for quark-quark and quark-antiquark scattering processes including $1/N_c$ next to leading order corrections as:

$$\tau^{-1} = 6f_0 \left(\bar{\sigma}_{uu \rightarrow uu} + \bar{\sigma}_{ud \rightarrow ud} + \bar{\sigma}_{u\bar{u} \rightarrow u\bar{u}} + \bar{\sigma}_{u\bar{u} \rightarrow d\bar{d}} + \bar{\sigma}_{u\bar{d} \rightarrow u\bar{d}} \right). \quad (\text{A6})$$

We refer the reader to Refs. [28, 94, 95] for details on the calculation of the $\bar{\sigma}'s$ – we note that the chiral model used in these references is not very different from the LSM, the exchanges of σ and π mesons are modeled by contact terms. Note also that the cross sections are temperature dependent, not only because of phase space, but also because they depend on the constituent quark masses, whose temperature dependence is given by the LSM of the present paper. See also Ref. [29] for a related approach applied to the calculation of η/s in the LSM of a pion gas.

Appendix B: Dependence of results on cut-off for η/s

It was noted before that any hydrodynamical description of matter is bound to become inapplicable at large viscosity. Since our simulations are purely hydrodynamic and the calculated η/s increases rapidly with decreasing temperature, a cut-off for the value of η/s must be imposed. The comparison of the results obtained from hydrodynamic and kinetic simulations to data provide a

guide as to what is the value at which one should impose the cut-off. In our simulations we set the cut-off at $\eta/s = 0.4$, which is in the range of values found to correspond to the breakdown of viscous hydrodynamics [50, 77]. In this Appendix we show the results for hadronic observables calculated using different values of this cut-off, namely $\eta/s \leq 0.3, 0.4$ and 0.5 , and analyse the dependence of the results on this choice for the cut-off. For simplicity, the results shown in this appendix correspond to $g = 3.2$.

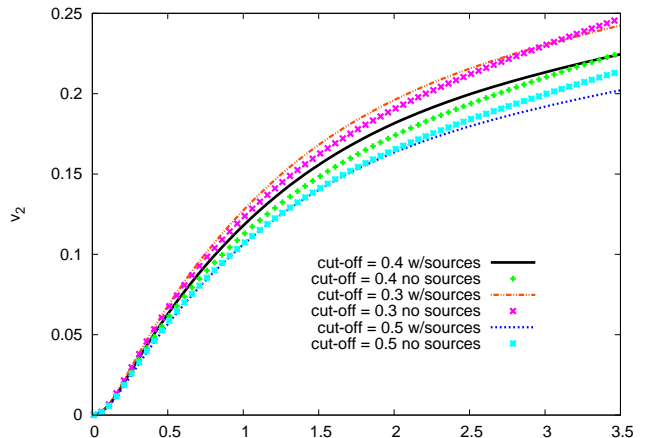


FIG. 8: (Color online) v_2 for charged-hadrons calculated taking or not taking into account the chiral fields as sources for the hydrodynamic equations calculated with different choices for the cut-off value $\eta/s = 0.3, 0.4, 0.5$. The value of the coupling constant is $g = 3.2$.

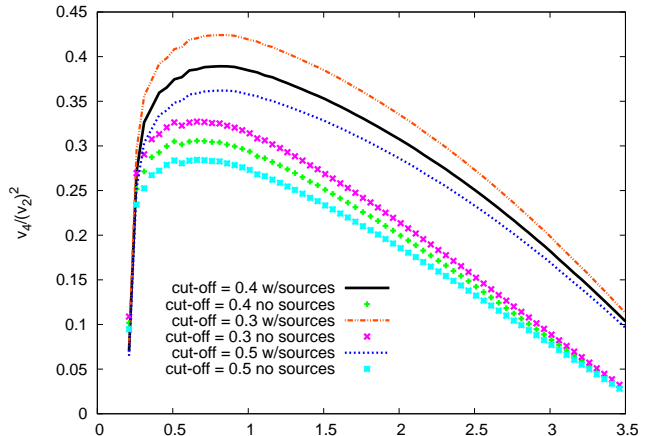


FIG. 9: (Color online) $v_4/(v_2)^2$ for charged-hadrons calculated taking or not taking into account the chiral fields as sources for the hydrodynamic equations calculated with different choices for the cut-off value $\eta/s = 0.3, 0.4, 0.5$. The value of the coupling constant is $g = 3.2$.

Figs. 8 and 9 show the charged-hadron v_2 and $v_4/(v_2)^2$, respectively, as a function of transverse momentum, obtained with cut-off values of $\eta/s = 0.3, 0.4$ and

0.5. It is seen that although the values of v_2 and $v_4/(v_2)^2$ change with the value of the cut-off, the relation between the results obtained including or not the chiral fields as sources in the hydrodynamic equations remains practically the same. Consequently, the conclusions extracted from these results, which are discussed in the main text, do not depend on the precise value of the cut-off imposed on η/s , provided that $g \sim 3.2$ corresponding to a smooth crossover.

As a final side remark, it is interesting to note that if one would attempt to extract the value of η/s by matching v_2 to data (with the remark mentioned in the Introduction), the uncertainty in the extracted η/s coming from the choice of cut-off in the range $[0.3, 0.5]$ would be $\sim 50\%$ with respect to the average value of η/s . This relatively large value of the uncertainty in η/s associated

with the imposed cut-off clearly displays the sensitivity of observables on the shear viscosity of the hadronic stage in collisions at $\sqrt{s_{NN}} = 200$ GeV, a fact already discussed in Refs. [8–11], pointing to the conclusion that further study is needed to extract the precise temperature dependence of η/s from heavy-ion collisions experiments.

Acknowledgments

We thank Jorge Noronha for useful comments on the calculation of transport coefficients of strongly coupled theories. This work was partially funded by CNPq and FAPESP (Brazilian agencies).

-
- [1] S. S. Adler, et al. (PHENIX Collaboration), Phys. Rev. Lett. **91**, 182301 (2003).
- [2] J. Adams, et al. (STAR Collaboration), Phys. Rev. Lett. **92**, 112301 (2004).
- [3] K. Adcox, et al. (PHENIX Collaboration), Phys. Rev. C **69**, 024904 (2004).
- [4] J. Adams, et al. (STAR Collaboration), Phys. Rev. C **72**, 014904 (2005).
- [5] I. Arsene, et al. (BRAHMS Collaboration), Phys. Rev. C **72**, 014908 (2005).
- [6] B. B. Back, et al. (PHOBOS Collaboration), Phys. Rev. C **72**, 051901(R) (2005).
- [7] J. -Y. Ollitrault, Phys. Rev. D **46**, 229 (1992).
- [8] H. Niemi, G. S. Denicol, P. Huovinen, E. Molnar, and D. H. Rischke, Phys. Rev. Lett. **106**, 212302 (2011).
- [9] J. L. Nagle, I. G. Bearden, W. A. Zajc, [arXiv:1102.0680 [nucl-th]].
- [10] C. Shen and U. W. Heinz, Phys. Rev. C **83**, 044909 (2011).
- [11] P. Bozek, Phys. Rev. C **81**, 034909 (2010).
- [12] G. S. Denicol, T. Kodama, and T. Koide, arXiv:1002.2394v1 [nucl-th].
- [13] J. R. Bhatt, H. Mishra, V. Sreekanth, JHEP **1011**, 106 (2010).
- [14] H. Song, U. W. Heinz, Phys. Rev. C **81**, 024905 (2010).
- [15] K. Kanaya, PoS **LATTICE2010**, 012 (2010).
- [16] A. Nakamura and S. Sakai, Phys. Rev. Lett. **94**, 072305 (2005).
- [17] H. B. Meyer, Phys. Rev. D **76** (2007) 101701.
- [18] H. B. Meyer, Phys. Rev. Lett. **100**, 162001 (2008).
- [19] P. B. Arnold, G. D. Moore, and L. G. Yaffe, J. High Energy Phys. **0011**, 001 (2000); **305**, 051 (2003).
- [20] P. B. Arnold, C. Dogan, and G. D. Moore, Phys. Rev. D **74**, 085021 (2006).
- [21] M. Prakash, M. Prakash, R. Venugopalan, and G. Welke, Phys. Rep. **227**, 321 (1993).
- [22] J. W. Chen and J. Wang, Phys. Rev. C **79**, 044913 (2009).
- [23] F. Wilczek, arXiv:hep-ph/0003183.
- [24] A. Dobado and F. J. Llanes-Estrada, Phys. Rev. D **69**, 116004 (2004).
- [25] A. Muronga, Phys. Rev. C **69**, 044901 (2004).
- [26] J.W. Chen, Y. H. Li, Y. F. Liu, and E. Nakano, Phys. Rev. D **76**, 114011 (2007).
- [27] K. Itakura, O. Morimatsu, and H. Otomo, Phys. Rev. D **77**, 014014 (2008).
- [28] C. Sasaki and K. Redlich, Phys. Rev. C **79**, 055207 (2009); *ibid.* Nucl. Phys. A **832**, 62 (2010).
- [29] P. Chakraborty and J. I. Kapusta, Phys. Rev. C **83**, 014906 (2011).
- [30] J. Noronha-Hostler, Jorge Noronha, and C. Greiner, Phys. Rev. Lett. **103**, 172302 (2009).
- [31] L. P. Csernai, J. I. Kapusta, and L. D. McLerran, Phys. Rev. Lett. **97**, 152303 (2006).
- [32] R. Baier, P. Romatschke, D. T. Son, A. O. Starinets, and M. A. Stephanov, J. High Energy Phys. **04** (2008) 100.
- [33] S. Bhattacharyya, V. E. Ehubeny, S. Minwalla, and M. Rangamani, J. High Energy Phys. **02** (2008) 045.
- [34] M. Natsuume and T. Okamura, Phys. Rev. D **77**, 066014 (2008); **78**, 089902(E) (2008).
- [35] M. Gell-Mann and M. Levy, Nuovo Cim. **16**, 705 (1960).
- [36] I.N. Mishustin and O. Scavenius, Phys. Rev. Lett. **83**, 3134 (1999).
- [37] A. Abada and M. C. Birse, Phys. Rev. D **55**, 6887 (1997).
- [38] D. T. Son, Phys. Rev. Lett. **84**, 3771 (2000).
- [39] C. Pujol and D. Davesne, Phys. Rev. C **67**, 014901 (2003).
- [40] Y. Lallouet, D. Davesne, and C. Pujol, Phys. Rev. C **67**, 057901 (2003).
- [41] K. Paech, H. Stöcker and A. Dumitru, Phys. Rev. C **68**, 044907 (2003).
- [42] K. Paech and A. Dumitru, Phys. Lett. B **623**, 200 (2005).
- [43] M. Nahrgang and M. Bleicher, J. Phys. Conf. Ser. **270**, 012059 (2010).
- [44] M. Nahrgang, S. Leupold, C. Herold, and M. Bleicher, [arXiv:1105.0622 [nucl-th]].
- [45] M. Nahrgang, S. Leupold, and M. Bleicher, [arXiv:1105.1396 [nucl-th]].
- [46] M. Nahrgang, M. Bleicher, S. Leupold, and I. Mishustin, [arXiv:1105.1962 [nucl-th]].
- [47] S. Plumari, V. Baran, M. Di Toro, G. Ferini, and V. Greco, Phys. Lett. B **689**, 18 (2010).
- [48] M. Luzum and P. Romatschke, Phys. Rev. C **78**, 034915 (2008); Erratum-*ibid.* C **79**, 039903 (2009).

- [49] U. W. Heinz, [arXiv:0901.4355 [nucl-th]].
- [50] P. Romatschke, *Int. J. Mod. Phys. E* **19**, 1 (2010);
- [51] J. Peralta-Ramos and E. Calzetta, *Phys. Rev. C* **82**, 054905 (2010).
- [52] R. P. G. Andrade, F. Grassi, Y. Hama, T. Kodama, W. L. Qian, *Phys. Rev. Lett.* **101**, 112301 (2008). [arXiv:0805.0018 [hep-ph]]
- [53] H. Petersen, C. Coleman-Smith, S. A. Bass, and R. Wolpert, *J. Phys. G* **38**, 045102 (2011).
- [54] R. S. Bhalerao, M. Luzum, and J.-Y. Ollitrault, arXiv:1104.4740v1 [nucl-th].
- [55] W. Israel, *Ann. Phys. (NY)* **100**, 310 (1976).
- [56] W. Israel and J. M. Stewart, *Phys. Lett. A* **58**, 213 (1976).
- [57] W. Israel and J. M. Stewart, *Ann. Phys. (NY)* **118**, 341 (1979).
- [58] B. Betz, D. Henkel, and D. H. Rischke, *J. Phys. G* **36**, 064029 (2009).
- [59] J. Noronha, and G. S. Denicol, arXiv:1104.2415v2 [hep-th].
- [60] G. S. Denicol, J. Noronha, H. Niemi, and D. H. Rischke, *Phys. Rev. D* **83**, 074019 (2011).
- [61] T. Koide and T. Kodama, *Phys. Rev. E* **78**, 051107 (2008).
- [62] F. Cooper and G. Frye, *Phys. Rev. D* **10**, 186 (1974).
- [63] S. R. de Groot, W. A. van Leeuwen and Ch. G. van Weert, *Relativistic Kinetic Theory* (North-Holland, Netherlands, 1980).
- [64] P. F. Kolb, J. Sollfrank, and U. Heinz, *Phys. Rev. C* **62**, 054909 (2000).
- [65] P. F. Kolb and R. Rapp, *Phys. Rev. C* **67**, 044903 (2003).
- [66] P.F. Kolb and U. Heinz, 0305084 [nucl-th]. AZHYDRO code v0.2 is available from <http://karman.physics.purdue.edu/OSCAR>.
- [67] W. Florkowski, *Nucl. Phys. A* **853**, 173 (2011).
- [68] M. Chojnacki and W. Florkowski, *Acta Phys. Polon. B* **38**, 3249 (2007).
- [69] S. Pratt, *Phys. Rev. Lett.* **102**, 232301 (2009).
- [70] Y. Aoki, G. Endrodi, Z. Fodor, S. D. Katz, and K.K. Szabo, *Nature* **443**, 675 (2006).
- [71] S. Borsanyi, Z. Fodor, C. Hoelbling, S. D. Katz, S. Krieg, C. Ratti, and K. K. Szabo, arXiv:1005.3508v1 [hep-lat].
- [72] R.A. Soltz (for the HotQCD Collaboration), *Nucl. Phys. A* **830**, 725 (2009).
- [73] M. Cheng, N. H. Christ, S. Datta, J. van der Heide, C. Jung, F. Karsch, O. Kaczmarek, E. Laermann, R. D. Mawhinney, C. Miao, P. Petreczky, K. Petrov, C. Schmidt, and T. Umeda, *Phys. Rev. D* **74**, 054507 (2006).
- [74] M. Laine and Y. Schroder, *Phys. Rev. D* **73**, 085009 (2006).
- [75] H. Song, S. A. Bass, and U. W. Heinz, *Phys. Rev. C* **83**, 024912 (2011).
- [76] D. Fernandez-Fraile and A. Gomez Nicola, arXiv:0912.4002v1 [hep-ph].
- [77] D. A. Teaney, arXiv:0905.2433v1 [nucl-th].
- [78] S. Pratt and G. Torrieri, *Phys. Rev. C* **82**, 044901 (2010).
- [79] H. Song and U. W. Heinz, *Phys. Rev. C* **81**, 024905 (2010).
- [80] A. Monnai, T. Hirano, *Phys. Rev. C* **80**, 054906 (2009).
- [81] P. Huovinen, D. Molnar, *Phys. Rev. C* **79**, 014906 (2009).
- [82] K. Aamodt, et al. (ALICE Collaboration), *Phys. Rev. Lett.* **107**, 032301 (2011).
- [83] C. Shen, S. A. Bass, T. Hirano, P. Huovinen, Z. Qiu, H. Song, U. W. Heinz, arXiv:1106.6350v1 [nucl-th].
- [84] B. Schenke, arXiv:1106.6012v1 [nucl-th].
- [85] J. L. Nagle and M. P. McCumber, *Phys. Rev. C* **83**, 044908 (2011).
- [86] R. A. Lacey, R. Wei, J. Jia, N. N. Ajitanand, and A. Taranenko, *Phys. Rev. C* **83**, 044902 (2011).
- [87] R. A. Lacey, R. Wei, N.N. Ajitanand, J.M. Alexander, X. Gong, J. Jia, A. Taranenko, R. Pak, H. Stöcker, *Phys. Rev. C* **81**, 061901 (2010).
- [88] M. Luzum, C. Gombeaud, and J.-Y. Ollitrault, *Phys. Rev. C* **81**, 054910 (2010).
- [89] M. Luzum and J.-Y. Ollitrault, *Phys. Rev. C* **82**, 014906 (2010).
- [90] E. Calzetta and J. Peralta-Ramos, *Phys. Rev. D* **82**, 106003 (2010).
- [91] K. Dusling, G. D. Moore, and D. Teaney, *Phys. Rev. C* **81**, 034907 (2010).
- [92] A. Monnai and T. Hirano, *Phys. Rev. C* **80**, 054906 (2009).
- [93] G. S. Denicol, T. Kodama, T. Koide, and Ph. Mota, *Phys. Rev. C* **80**, 064901 (2009).
- [94] P. Zhuang, J. Hufner, S. P. Klevansky, and L. Neise, *Phys. Rev. D* **51**, 3728 (1995).
- [95] P. Rehberg, S. P. Klevansky, and J. Hufner, *Nucl. Phys. A* **608**, 356 (1996).